Phase diagram of the frustrated spin ladder

Toshiya Hikihara[1] and Oleg A. Starykh[2]
[1]*Department of Physics, Hokkaido University, Sapporo 060-0810, Japan*
[2]*Department of Physics and Astronomy, University of Utah, Salt Lake City, Utah 84112, USA*
(Received 20 December 2009; revised manuscript received 29 January 2010; published 25 February 2010)

We revisit the phase diagram of the frustrated spin-1/2 ladder with two competing interchain antiferromagnetic exchanges, rung coupling $J_\perp$ and diagonal coupling $J_\times$. We suggest, based on the accurate renormalization-group analysis of the low-energy Hamiltonian of the ladder, that marginal interchain current-current interaction plays central role in destabilizing previously predicted intermediate columnar dimer phase in the vicinity of classical degeneracy line $J_\perp=2J_\times$. Following this insight we then suggest that changing these competing interchain exchanges from the previously considered antiferromagnetic to the *ferromagnetic* ones eliminates the issue of the marginal interactions altogether and dramatically expands the region of stability of the *columnar dimer phase*. This analytical prediction is convincingly confirmed by the numerical density-matrix renormalization-group and exact-diagonalization calculations as well as by the perturbative calculation in the strong rung-coupling limit. The phase diagram for ferromagnetic $J_\perp$ and $J_\times$ is determined.

DOI: 10.1103/PhysRevB.81.064432 PACS number(s): 75.10.Jm, 75.10.Pq, 75.30.Kz, 75.40.Cx

I. INTRODUCTION

Frustrated quantum antiferromagnets have for a long-time attracted attention of both theorists and experimentalists.[1] One of the main reasons for this continuing focus is the dominant role of quantum fluctuations in stabilizing various classical and quantum orders in this class of systems. Spin ladders represent particularly interesting class of models exhibiting rich variety of phases.[2–6] In addition to being interesting in their own right, spin ladders allow for high precision numerical investigations by density-matrix renormalization group (DMRG) (Refs. 7 and 8) and quantum Monte Carlo techniques. One of the most striking features of spin ladders consists in the finding[2] that generic interchain interaction flows toward strong coupling, resulting in a confinement of gapless spin-1/2 spinon excitations of constituent spin chains (which form legs of the ladder) into tightly bound spin-1 pairs (triplons). Extensive experimental efforts[9] resulted in observation of one- and even two-triplons states in $La_4Sr_{10}Cu_{24}O_{41}$.[10] Most recently, an evolution of spin excitations from those of deconfined spinons at high energies to bound triplet and singlet spinon pairs at low energies has been mapped via inelastic neutron scattering in the weakly coupled ladder material $CaCu_2O_3$.[11]

While the standard ladder geometry realizes interchain interaction between spins on the legs in the form of nonfrustrated exchange along the rungs of the ladder, a more complicated geometry is possible as well. In this work we focus on the ladder with *frustrated* interchain interactions between leg spins, when the interchain exchange takes place both on rungs [Eq. (3) below] and diagonals [Eq. (4)]. Such geometry is, in fact, typical for many spin-chain materials where the superexchange between spins proceeds via 90° Cu-O bonds. In particular, well-studied spin-chain oxides $SrCuO_2$ and Sr_2CuO_3 are characterized by the presence of (very weak) rung and diagonal exchanges,[12] which frustrate correlations between chain spins and leads to extremely low three-dimensional ordering temperatures.

In this work, we revisit and resolve one of the outstanding questions in this field—the appearance of spontaneously dimerized ground state in frustrated spin-ladder model with only pairwise exchange interactions between microscopic lattice spins. Specifically, the Hamiltonian of the problem reads

$$H = H_{\text{leg}} + H_{\text{rung}} + H_{\text{diag}}, \tag{1}$$

where

$$H_{\text{leg}} = J\sum_n (\mathbf{S}_{1,n}\cdot\mathbf{S}_{1,n+1} + \mathbf{S}_{2,n}\cdot\mathbf{S}_{2,n+1}) \tag{2}$$

describes two isotropic Heisenberg chains with positive (antiferromagnetic) nearest-neighbor exchange J while

$$H_{\text{rung}} = J_\perp\sum_n \mathbf{S}_{1,n}\cdot\mathbf{S}_{2,n} \tag{3}$$

and

$$H_{\text{diag}} = J_\times\sum_n (\mathbf{S}_{1,n}\cdot\mathbf{S}_{2,n+1} + \mathbf{S}_{2,n}\cdot\mathbf{S}_{1,n+1}) \tag{4}$$

describe frustrated interchain interaction $H_{\text{inter}}=H_{\text{rung}}+H_{\text{diag}}$.

In the weak-coupling limit ($J_\perp, J_\times \ll J$) one treats interchain interaction H_{inter} as a perturbation and takes continuum limit along the chain direction. It is then easy to see that for $J_\perp<2J_\times$ the ground state is of Haldane type, with two spin-1/2 on the rung forming effective spin-1, while for $J_\perp>2J_\times$ rung pairs form singlets, resulting in the rung-singlet (RS) phase. Transition region $J_\perp\approx 2J_\times$ between these two well-understood phases requires careful analysis which is described in Ref. 13. It was found there that in the narrow region (boundaries are approximate)

$$2J_\times - \frac{5J_\times^2}{\pi^2 J} < J_\perp < 2J_\times - \frac{J_\times^2}{\pi^2 J}, \tag{5}$$

the ladder should exhibit *columnar dimer* (CD) phase in its ground state.[13] This finding was questioned in several extensive numerical studies[14,15] which suggested that the CD phase is absent and that instead there is a direct transition between Haldane ($J_\perp<2J_\times$) and RS ($J_\perp>2J_\times$) ground

states. The most recent work[16] on this subject does find the dimerized phase, although the evidence for this is not particularly strong.

Narrow extent [Eq. (5)] of the suggested CD order makes numerical analysis of the problem difficult. We will argue below that in the case of *antiferromagnetic* couplings, $J_\perp, J_\times > 0$, the situation is even more complicated by the presence of marginally relevant interchain interaction between spin currents (uniform magnetization) of the two chains. We show that this interaction is responsible for suppressing the CD instability for not too small interchain exchange values ($J_\perp \geq 0.3J$ or so) and producing the first-order phase transition between the Haldane and RS phases instead. We also show that changing the *sign* of the interchain couplings to a *ferromagnetic* one (so that $J_\perp, J_\times < 0$) effectively removes the current-current interaction from the problem and allows one to access the CD phase even for not too small $|J_{\perp,\times}|$ values. These arguments, derived from renormalization group (RG) analysis described in Sec. II, are supported by extensive DMRG and exact-diagonalization calculations as well as the perturbation analysis for the strong rung-coupling limit, results of which are reported in Sec. III. The ground-state phase diagram in the $J_\perp$-$J_\times$ plane for the ferromagnetic case is also presented there. The case of antiferromagnetic couplings between chains of the ladder is addressed again in Sec. IV. We conclude by summarizing our findings in Sec. V. Appendix describes an application of our numerical approach to the well-understood case of a single frustrated Heisenberg chain which is known to realize the spontaneously dimerized ground state.

II. RG ANALYSIS

Low-energy description of the problem is based on the continuum representation of the spin operator

$$\mathbf{S}_n/a_0 = \mathbf{M}(x) + (-1)^x \mathbf{N}(x), \tag{6}$$

where $x = na_0$ and a_0 is the lattice spacing, which we set to unity in what follows. Uniform $\mathbf{M}$ and staggered $\mathbf{N}$ magnetizations represent spin fluctuations with momenta near $q=0$ and π/a_0, correspondingly. Another very important for the following low-energy degree of freedom is staggered dimerization $\epsilon(x)$. It represents fluctuational part of the bond strength (energy density) between two neighboring spins on the chain,

$$\epsilon(x) = (-1)^x (\mathbf{S}_n \cdot \mathbf{S}_{n+1} - C_{\mathrm{av}}). \tag{7}$$

The second term, C_{av}, represents an *average* energy per bond, which is a position-independent constant. Spontaneously dimerized ground state is characterized by the finite expectation value of dimerization, $\langle \epsilon \rangle$, which describes the staggered pattern of strong and weak bonds along the chain.

Low-energy limit of the interchain Hamiltonian is then found to contain at least five couplings that flow under RG.

$$H_{\mathrm{inter}} = \int dx (g_1 N + g_2 J + g_3 a^2 M + g_4 E + g_5 K), \tag{8}$$

where we introduced the following short-hand notations:

$$N = \mathbf{N}_1 \cdot \mathbf{N}_2, \quad J = \mathbf{M}_{1R} \cdot \mathbf{M}_{2L} + \mathbf{M}_{1L} \cdot \mathbf{M}_{2R},$$

$$M = \partial_x \mathbf{N}_1 \cdot \partial_x \mathbf{N}_2, \quad E = \epsilon_1 \epsilon_2,$$

$$K = \mathbf{M}_{1R} \cdot \mathbf{M}_{1L} + \mathbf{M}_{2R} \cdot \mathbf{M}_{2L} \tag{9}$$

The relevant couplings are $g_{1,4}$ which describe coupling between staggered magnetizations $\mathbf{N}_j$ and staggered dimerizations ϵ_j of the chains, correspondingly. Marginal couplings include g_2 and g_5, which describe current-current interaction between chains (g_2) as well as residual (and naively, marginally irrelevant) in-chain backscattering (g_5). The irrelevant terms contain g_3, which is of key importance for generating (together with g_2) the novel $\epsilon_1 \epsilon_2$ term (coupling g_4 above). This term should be, strictly speaking, be supplemented with $g_6 \partial_x \epsilon_1 \partial_x \epsilon_2$ which will certainly be generated (as well as other more irrelevant terms)—but its small initial value, $\sim J_{\perp,\times}^2/J$, allows us to neglect it. Initial values of the couplings are:

$$g_1(0) = J_\perp - 2J_\times, \quad g_2(0) = J_\perp + 2J_\times, \quad g_3(0) = J_\perp/2,$$

$$g_4(0) = 0, \quad g_5(0) = -0.23(2\pi v). \tag{10}$$

The value of $g_5(0)$ has been estimated in Ref. 17. RG equations for our model[13,15] are rather similar to the much studied case of the zigzag ladder.[18] They are conveniently formulated in terms of dimensionless variables

$$G_{1,3,4} = \frac{g_{1,3,4}\lambda^2}{2\pi v}, \quad G_{2,5} = \frac{g_{2,5}}{2\pi v} \tag{11}$$

and read ($\dot{g} = dg/d\ell$, where ℓ is the RG scale)

$$\dot{G}_1 = G_1 + G_1 G_2 - \frac{1}{2} G_1 G_5 + G_2 G_3 - \frac{1}{2} G_2 G_4,$$

$$\dot{G}_2 = G_2^2 + 4G_1^2 + 4G_1 G_3 - 4G_1 G_4 - 2G_3 G_4,$$

$$\dot{G}_3 = -G_3,$$

$$\dot{G}_4 = G_4 - \frac{3}{2} G_1 G_2 - \frac{3}{2} G_2 G_3 + \frac{3}{2} G_4 G_5,$$

$$\dot{G}_5 = G_5^2 - 2G_1^2 + 2G_1 G_3 + 2G_4^2. \tag{12}$$

Almost everywhere in parameter space $(J_\perp, J_\times)$ $g_{1,4}$ diverge exponentially while g_3 dies off exponentially and the flow is completely determined by the initial value of $g_1(0)$ [remember that $g_4(0)=0$]. But in the vicinity of $J_\perp = 2J_\times$ line things are different because naively there $g_1(0)=0$ as well. Thus there two relevant operators appear to be absent due to fine tuning. This region requires careful study.

Let us assume that we are very close to this line so that $G_1(0) = O(J_\times^2/J^2)$. Note that other couplings are $G_{2,3}(0) = O(J_\times/J)$ because they are not sensitive to the difference $J_\perp - 2J_\times$. In order to understand how the flow starts consider very short RG times, $\ell \leq \ell_0 = 1$ and keep only terms of order $(J_\times/J)^2$ in the right-hand side of the RG equations. The system simplifies dramatically and we find that $G_{2,3,5}$

"decouple" from the equations for the relevant $G_{1,4}$ couplings

$$G_2(\ell) = G_2(0)/[1 - G_2(0)\ell],$$

$$G_3(\ell) = G_3(0)e^{-\ell},$$

$$G_5(\ell) = G_5(0)/(1 + |G_5(0)|\ell) \to -1/\ell. \tag{13}$$

Thus for $\ell \sim 1$ we have

$$\dot{G}_1 = G_1 + G_2 G_3,$$

$$\dot{G}_4 = G_4 - \frac{3}{2} G_2 G_3. \tag{14}$$

Note that for such short ℓ's we can safely treat marginal couplings $G_{2,5}$ as constants, because $G_{2,5}(0) \ll 1$. The last two equations then admit straightforward solution

$$G_1(\ell) = \left(G_1(0) + \frac{q}{2}\right)e^{\ell} - \frac{q}{2}e^{-\ell},$$

$$G_4(\ell) = \frac{-3q}{2}\sinh[\ell], \tag{15}$$

where $q \equiv G_2(0)G_3(0) = (2J_\times/2\pi v)^2 = (2J_\times/\pi^2 J)^2$, and we made use of the initial condition $G_4(0) = 0$ and of the fact that the spin velocity is given by $v = \pi J/2$. We observe renormalization of the initial values of $G_{1,4}$ couplings by quantum fluctuations. It is clear that for intermediate range of $0 < \ell \ll \ell_1 = \ln(J/J_\times)$, where the approximation Eq. (14) is expected to work, the two Eqs. (15) describe evolution of relevant $G_{1,4}$ couplings with initial values given by $G_1(0) \to G_1(0) + q/2$ and $G_4(0) \to -3q/4$, correspondingly. The same renormalization can be obtained via direct perturbative calculation, as was done originally in Ref. 13.

Once $G_{1,4}$ got some nonzero initial values of the order $(J_\times/J)^2$, they will grow exponentially fast and at $\ell_1 \sim \ln(J/J_\times) \ll \ell_2 = 1/G_2(0) \sim J/J_\times$ reach values of the order $J_\times/J$. Note that $G_2(\ell_1) \sim J_\times/J \ll 1$ at this scale and our weak-coupling consideration still makes sense. An estimate of the range where the dimerized phase is expected to appear, *neglecting* the flow of the marginal couplings, can now be obtained with the help of refermionization procedure as described in Ref. 13. Specifically, the model Eq. (8) with two competing relevant couplings g_1 and g_4 maps onto the theory of four (weakly interacting) Majorana fermions which are organized into a *triplet* with mass $m_t \propto 2\pi v(G_1 - G_4)$ and a *singlet* with mass $m_s \propto -2\pi v(3G_1 + G_4)$. The Haldane-to-CD transition corresponds to the vanishing of the triplet mass, $m_t = 0$, and takes place when $J_\perp - 2J_\times + 5J_\times^2/(\pi^2 J) = 0$. The CD-to-RS transition is described by the condition $m_s = 0$ and results in $J_\perp - 2J_\times + J_\times^2/(\pi^2 J) = 0$. Putting these two boundaries together leads to the estimate Eq. (5).

The neglect of the marginal terms, and in particular of the interchain current-current one, G_2, is well justified in the asymptotic limit $J_{\perp,\times}/J \to 0$. Away from this limit, but still keeping $J_{\perp,\times}/J \ll 1$, one has to be mindful of the marginally relevant character of G_2 term in the case of *antiferromagnetic* (positive) sign of exchanges $J_{\perp,\times}$. Left alone, G_2 would diverge at $\ell \sim J/J_\times$, as follows from Eq. (13). It may happen that for not too small $J_{\perp,\times}/J$ the marginal coupling G_2 reaches value of the order 1 before the relevant couplings $G_{1,4}$ do so. In the following we denote the corresponding RG scale as ℓ_3: thus $G_2(\ell_3) \approx 1$ while $G_{1,4}(\ell_3) < 1$.

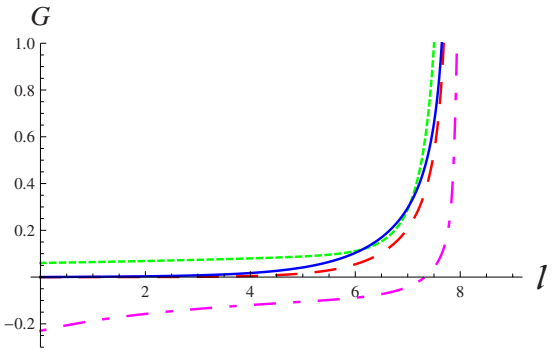

FIG. 1. (Color online) RG flow of couplings $G_{1,2,4,5}$ for the case of antiferromagnetic interchain exchanges $J_\times = 0.15$ and $J_\perp = 0.296$. Notations are as follows: G_1 (red/dashed), G_2 (green/dotted), $-G_4$ (blue/solid), and G_5 (magenta/dot-dashed). ℓ denotes RG scale.

Such a behavior implies direct first-order transition between Haldane and RS phases,[13,19–21] which can be analyzed with the help of abelian bosonization along the lines sketched previously in Ref. 13. In terms of conjugate bosonic fields φ_m and θ_m, where $m = \pm$ denotes symmetric/antisymmetric combination of the original chain fields, the interchain interaction Eq. (8) acquires the form

$$H'_{\text{inter}} = \frac{1}{2\pi^2 a_0^2}\int dx[g_2 \cos(\sqrt{4\pi}\varphi_+)\cos(\sqrt{4\pi}\theta_-) + 2g_1 \cos(\sqrt{4\pi}\theta_-) - (g_1 - g_4)\cos(\sqrt{4\pi}\varphi_+) + (g_1 + g_4)\cos(\sqrt{4\pi}\varphi_-)]. \tag{16}$$

This expression includes only relevant and marginally relevant terms of Eq. (8) (i.e., terms N, E, and J) *evaluated* at $\ell = \ell_3$. The two remaining terms (M and K) are omitted because of their irrelevancy at this late stage of RG development. In the regime we are interested here $g_2 \gg g_{1,4}$, which implies that H'_{inter} is minimized by (a) $\varphi_+ = \sqrt{\pi}/2$, $\theta_- = 0$ and (b) $\varphi_+ = 0$, $\theta_- = \sqrt{\pi}/2$. The first choice describes Haldane state while the second corresponds to the RS one, see Ref. 13. Since θ_- is pinned in both states, the last term in Eq. (16) effectively averages to zero, $\cos[\sqrt{4\pi}\varphi_-] \to 0$. Treating the remaining two terms as a perturbation, we find that $g_4 = 3g_1$ describes a *first-order transition* line separating Haldane and RS phases. Everywhere on this line the energies of the two states are equal. Line's end points can be estimated as points where $g_2 = g_{1,4}$, see Ref. 13 and Fig. 1 therein. Since the Haldane and the RS states are degenerate on the first-order transition line, elementary excitations on this line are (massless) domain walls or kinks, interpolating between vacua of types (a) and (b) above. The spin of such a kink can be evaluated as

$$S^z_{\text{total}} = S^z_1 + S^z_2 = \partial_x(\varphi_1 + \varphi_2)/\sqrt{2\pi} = \partial_x\varphi_+/\sqrt{\pi}. \quad (17)$$

Assuming, for example, $\varphi_+(x=-\infty)=0$ and $\varphi_+(x=+\infty)=\sqrt{\pi}/2$, we find $S^z_{\text{total}}=1/2$: the kink is a *spinon*![21] These spinons can be visualized as spin-1/2 end states of the Haldane phase segments—since the length of the segment is arbitrary, the spinons are mobile and massless.[13] Away from the line $g_4=3g_1$ the spinons are bound into pairs as the energy cost of two distant kinks is proportional to the length of "minority" phase segment between them.

Once the initial parameters are such that one of the relevant couplings $g_{1,4}$ reaches 1 before the marginal g_2, the intermediate phase separating Haldane and RS phases becomes unavoidable. For positive g_4 such intermediate phase realizes *staggered dimer* (SD) phase ($\varphi_+=\sqrt{\pi}/2$, $\varphi_-=\sqrt{\pi}/2$) while *negative* g_4 results in the CD phase ($\varphi_+=0$, $\varphi_-=0$) which is the focus of this work. Such a situation is realized in the strict weak-coupling limit, $J_{\perp,\times}/J\to 0$, when the relevant couplings are certain to flow to values of order one well before any of the marginal ones can do so—and thus we once again conclude that dimerized phase is unavoidable. Its numerical detection is, however, very challenging in this very limit.

Solving full system of RG Eq. (12) numerically we find that conditions favoring the direct first-order transition are realized for (approximately) $J_\times \geq J^*_\times \approx 0.3$ and $J_\perp \approx 2J_\times$. Even though it is not *a priori* clear that our weak-coupling theory can adequately describe these somewhat large interchain couplings, observation of the direct transition between Haldane and RS states in several numerical studies suggests that analytical description based on Eqs. (12) and (16) remains valid there. We thus conclude that antiferromagnetically coupled frustrated ladder should exhibit CD phase in the range approximately given by Eq. (5) and for *not too large* interchain exchanges, $J_\times \leq J^*_\times$. Stronger interchain exchange leads to the collapse of the CD phase and direct first-order transition between Haldane and RS ground states. The situation is very similar to the phase diagram of the extended Hubbard model,[22–24] where one finds that charge-density-wave and spin-density-wave phases are separated by the bond-charge-density-wave phase. This intermediate phase collapses and gets replaced by the line of direct first-order transition once Hubbard repulsion constant exceeds some critical value.

The outlined reasoning suggests simple way to avoid the marginal interaction issue altogether: all we need to do is to change the signs of both interchain exchanges to the *ferromagnetic* (negative) ones. This simple change *preserves* frustrated nature of the interchain couplings—large negative $J_\perp$ leads to an effective spin-1 chain and the Haldane phase while large negative $J_\times$ forces rung spins into the RS phase. Importantly, this change makes interchain G_2 *marginally irrelevant* so that $G_2(\ell)=G_2(0)/(1+|G_2(0)|\ell)\to -1/\ell$ (neglecting for a moment effect of all other couplings). In effect, this simple sign change sends the scale ℓ_3 to infinity, $\ell_3\to\infty$. We now should be able, within the weak-coupling approximation, to get rid of G_2, which forces the CD phase to shrink, without suppressing the all-important competition between G_1 and G_4 terms. This is indeed observed in numerical solution of the system Eq. (12). The difference between antiferromagnetic and ferromagnetic interchain couplings is illustrated in Figs. 1 and 2. Coupling G_2, shown by dotted (green) line there, overtakes relevant $G_{1,4}$ on the way to strong coupling in Fig. 1 (antiferromagnetic case) while it remains small in Fig. 2 (ferromagnetic case).

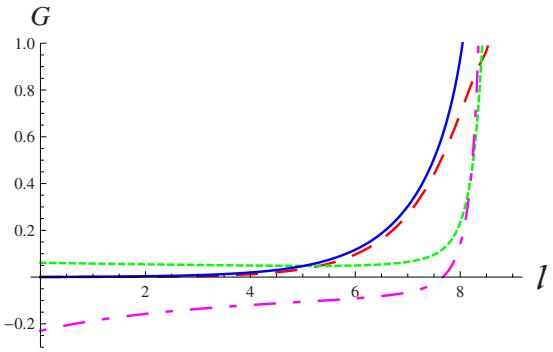

FIG. 2. (Color online) RG flow of couplings $G_{1,2,4,5}$ for the case of ferromagnetic interchain exchanges $J_\times=-0.15$ and $J_\perp=-0.306$. Notations are as follows: $-G_1$ (red/dashed), $-G_2$ (green/dotted), $-G_4$ (blue/solid), and G_5 (magenta/dot-dashed). ℓ denotes RG scale.

Results of numerical solutions for some sample values of $J_{\times,\perp}$ are summarized in the Table I, which shows that making the interchain exchanges ferromagnetic indeed helps one to unmask the novel columnar dimer phase.

III. FERROMAGNETIC INTERCHAIN COUPLINGS

Motivated by the result of RG analysis in Sec. II, we study the case of ferromagnetic interchain couplings $J_\perp$, $J_\times<0$. First, we treat the limit of strong rung coupling, $|J_\perp| \gg J, |J_\times|$, and show that for $J+J_\times=0$ the model exhibits

TABLE I. Brief summary of numerical solution of RG system Eq. (12) for several values of $J_\times$. Positive (negative) values of $J_{\times,\perp}$ correspond to antiferromagnetic (ferromagnetic) interchain exchanges. Second (third) column describes the range of $J_\perp$ for which the columnar dimer phase is realized according to Eq. (12) [Eq. (5)]. Last column shows the most divergent coupling constant which reaches value of order one first.

$J_\times$	Range of $J_\perp$ [Eq. (12)]	Estimate of $J_\perp$ [Eq. (5)]	Leading g
0.05	(0.09945, 0.09955)	(0.0987, 0.0997)	g_4
0.1	(0.1978, 0.1982)	(0.1949, 0.1990)	g_4
0.15	(0.295, 0.2956)	(0.2886, 0.2977)	g_4
0.2	(0.39096, 0.392)	(0.3797, 0.3959)	g_4
0.3	none	(0.5544, 0.5909)	g_2
0.4	none	(0.7189, 0.7838)	g_2
0.5	none	(0.8733, 0.9747)	g_2
−0.15	(−0.303, −0.3062)	(−0.3023, −0.3114)	g_4
−0.3	(−0.608, −0.635)	(−0.6091, −0.6456)	g_4
−0.4	(−0.815, −0.882)	(−0.8162, −0.8811)	g_4
−0.5	(−1.02, −1.16)	(−1.025, −1.127)	g_4

the CD long-range order. We then present our numerical DMRG and exact-diagonalization data for the model. Combining the results, we determine the ground-state phase diagram, which includes the CD phase in a wide parameter range between the Haldane and RS phases.

A. Strong rung-coupling limit

We consider the limit of strong rung coupling, $|J_\perp| \gg J, |J_\times|$. We first diagonalize the rung Hamiltonian $H_{\rm rung}$, whose ground states are a direct product of triplet states in each rung. We then include the effect of $H_{\rm leg}$ and $H_{\rm diag}$ perturbatively. It is convenient to rewrite the perturbation term as

$$H' = H_{\rm leg} + H_{\rm diag} = \frac{1}{2}(J+J_\times)\sum_n (\mathbf{S}_{1,n}+\mathbf{S}_{2,n})\cdot(\mathbf{S}_{1,n+1} + \mathbf{S}_{2,n+1}) + \frac{1}{2}(J-J_\times)\sum_n (\mathbf{S}_{1,n}-\mathbf{S}_{2,n})\cdot(\mathbf{S}_{1,n+1}-\mathbf{S}_{2,n+1}). \quad (18)$$

Note that the first term preserves the total spin in each rung while the second term changes the rung-triplet state to rung-singlet one and vice versa.

When $J+J_\times \neq 0$, the calculation is easy. The first term in Eq. (18) gives a nonzero contribution at the first-order perturbation and lifts the ground-state degeneracy of $H_{\rm rung}$. The effective Hamiltonian turns out to be the spin-1 Heisenberg chain,

$$\tilde{H}^{(1)} = \tilde{J}^{(1)}\sum_n \tilde{\mathbf{S}}_n \cdot \tilde{\mathbf{S}}_{n+1}, \quad (19)$$

where $\tilde{\mathbf{S}}_n$ is the spin-1 operator consisting of rung spins $\mathbf{S}_{1,n}$ and $\mathbf{S}_{2,n}$ and $\tilde{J}^{(1)}=(J+J_\times)/2$. Therefore, if $J+J_\times>0$, the system is in the Haldane phase while the system exhibits the ferromagnetic ground state for $J+J_\times<0$.

For $J+J_\times=0$, the first-order perturbation vanishes, and we must turn to the second order. From a straightforward calculation, we obtain the second-order perturbation Hamiltonian of the form,

$$\tilde{H}^{(2)} = \tilde{J}^{(2)}\sum_n [(\tilde{\mathbf{S}}_n \cdot \tilde{\mathbf{S}}_{n+1})^2 - 1] \quad (20)$$

with

$$\tilde{J}^{(2)} = -\frac{1}{8|J_\perp|}(J-J_\times)^2 = -\frac{J^2}{2|J_\perp|} = -\frac{J_\times^2}{2|J_\perp|}. \quad (21)$$

Therefore, the low-energy physics of the system is described by the spin-1 pure biquadratic chain with negative $\tilde{J}^{(2)}$. For this case it has been established that the model has the dimerized ground state.[25–30] Hence, mapping the spin-1 dimerized phase back to our model, we conclude that the spin-1/2 two-leg frustrated ladder Eq. (1) must exhibit CD phase along the line $J_\times=-J$ in the strong rung-exchange limit.

B. DMRG results

To search for the CD state and determine the ground-state phase diagram, we carry out the DMRG calculation[31,32] for the frustrated ladder Eq. (1). The calculation is performed for the system with up to $L=192$ rungs. For the efficiency of the DMRG method, the open boundary condition is imposed in the calculation. The number of kept states are typically $m=350$ for $L\leq 96$, $m=400$ for $L=128$, 192, and up to $m=500$ for some cases of the severe truncation error. We have monitored the truncation error of the data by comparing the results obtained with different m's and confirmed that the m convergence has been achieved for the data shown in the following.

To detect the CD order, we calculate the local CD operator in the open ladder with L rungs,

$$D_{\rm CD}(n;L) = \sum_{j=1,2} (\langle \mathbf{S}_{j,n}\cdot\mathbf{S}_{j,n+1}\rangle - \langle \mathbf{S}_{j,n+1}\cdot\mathbf{S}_{j,n+2}\rangle), \quad (22)$$

where $\langle\cdots\rangle$ denotes the expectation value in the ground state, i.e., the lowest-energy state in the subspace of zero magnetization $S^z_{\rm tot}=\Sigma_{j,n}S^z_{j,n}=0$. In the CD phase, the CD order induced at open boundaries of the ladder penetrates into the bulk and exhibits a long-range order. In the other phases with a spin gap, the CD order is expected to decay exponentially when we move from the boundary into the bulk, while we expect that the CD order decays algebraically at a critical point. We may therefore be able to identify the CD phase and transition points by monitoring the system-size dependence of the CD operator $D_{\rm CD}(n;L)$ at the center of open ladder, $n=L/2$. In the calculation, we set L to be a multiple of four so that $D_{\rm CD}(L/2;L)$ is positive.

Figure 3 shows the dependence of the CD operator $D_{\rm CD}(L/2;L)$ on the rung coupling $J_\perp$ for $J=1$ and several fixed $J_\times$. We find that $D_{\rm CD}(L/2;L)$ has a broad peak, indicating that the CD order is strong in a rather wide regime of $J_\perp$. We note that for $J_\times=-1$ and $J_\perp\lesssim -2$, the L convergence of $D_{\rm CD}(L/2;L)$ seems almost achieved, suggesting the appearance of the CD long-range order.

In order to determine whether or not the CD order survives in the thermodynamic limit, we investigate the system-size dependence of the CD operator $D_{\rm CD}(L/2;L)$. Figure 4 shows the L dependence of the CD operator $D_{\rm CD}(L/2;L)$ for some typical sets of coupling parameters. It is clear that $D_{\rm CD}(L/2;L)$ for $J_\times=-1$ and large negative $J_\perp$ converges to a finite value at $L\to\infty$.

We also show in Fig. 5 the spatial profile of the nearest-neighbor spin correlations $\langle \mathbf{S}_{j,n}\cdot\mathbf{S}_{j,n+1}\rangle = C_{\rm av}+(-1)^n\langle\epsilon_n\rangle$ for $(J,J_\times,J_\perp)=(1,-1,-3)$, which clearly demonstrates the presence of well-developed columnar dimer order. The average energy density, calculated in the middle of the ladder, is found to be $C_{\rm av}=(\langle \mathbf{S}_{j,L/2-1}\cdot\mathbf{S}_{j,L/2}\rangle+\langle \mathbf{S}_{j,L/2}\cdot\mathbf{S}_{j,L/2+1}\rangle)/2 = -0.384$. We see strong modulation of the bond energy $\langle \mathbf{S}_{j,n}\cdot\mathbf{S}_{j,n+1}\rangle$ between even and odd bonds. The amplitude of the modulation saturates in the middle of the ladder where the bulk dimerization value is achieved, $\langle\epsilon_n\rangle\to 0.136$. We find that bond modulations in the two chains are in phase, implying *columnar* ordering of stronger and weaker bonds. This finding represents direct proof of the CD phase in the frustrated ladder model Eq. (1) with ferromagnetic interchain exchanges.

For smaller $|J_\times|$, on the other hand, the appearance of the CD long-range order is not so clear; $D_{\rm CD}(L/2;L)$ still de-

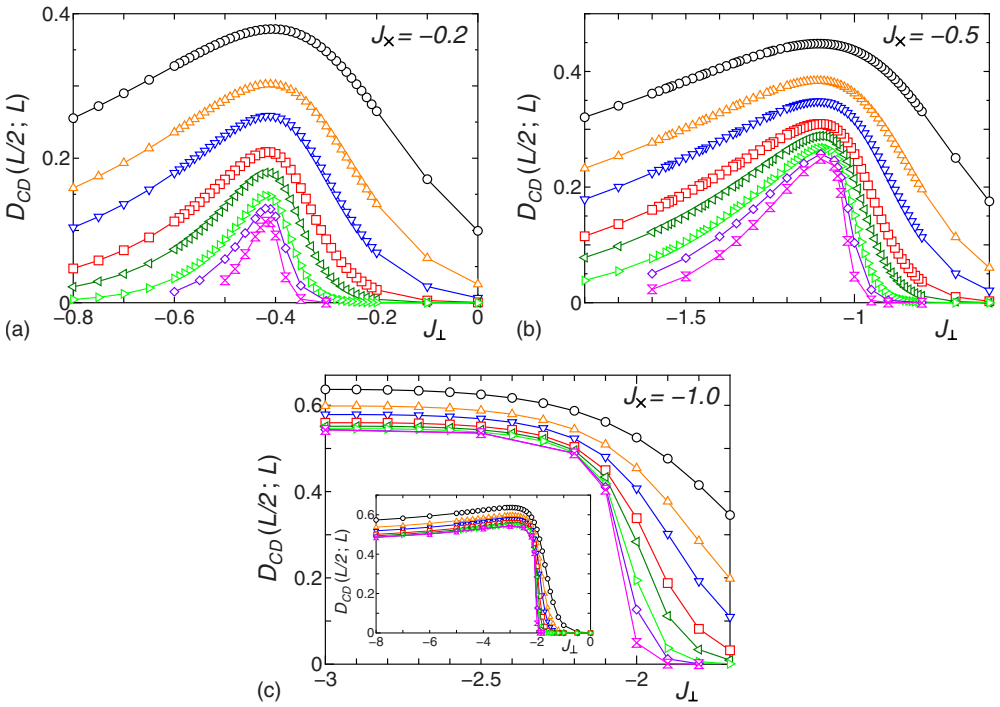

FIG. 3. (Color online) CD operator at the center of the open ladder, $D_{\mathrm{CD}}(L/2;L)$ as a function of $J_\perp$ for $J=1$ and (a) $J_\times=-0.2$, (b) $J_\times=-0.5$, and (c) $J_\times=-1.0$. The symbols represent the data for $L=16$, 24, 32, 48, 64, 96, 128, and 192 from top to bottom. Inset in (c) shows the data for $J_\times=-1.0$ and broader regime of $J_\perp$, $-8\leq J_\perp\leq 0$.

creases with L even at the largest L calculated [see Figs. 4(a) and 4(b)]. However, we find that in some parameter regime $D_{\mathrm{CD}}(L/2;L)$ *bends upward* in a log-log plot. This means that the decay of $D_{\mathrm{CD}}(L/2;L)$ becomes slower as L gets larger, which suggests the emergence of the CD long-range order in the thermodynamic limit.

To elucidate the bending-up behavior, we also investigate the system-size dependence of the slope of the log-log plot,

$$\Delta_{\mathrm{CD}}(x_i) = \frac{\log[D_{\mathrm{CD}}(L_{i+1}/2;L_{i+1})] - \log[D_{\mathrm{CD}}(L_i/2;L_i)]}{\log(L_{i+1}) - \log(L_i)}, \tag{23}$$

where $x_i=(L_i+L_{i+1})/2$ and $L_i=16,24,32,48,64,96,128,192$ for $i=1,2,\ldots,8$. If $D_{\mathrm{CD}}(L/2;L)$ decays exponentially with increasing L, the slope $\Delta_{\mathrm{CD}}(x)$ decreases as x increases. If $D_{\mathrm{CD}}(L/2;L)$ exhibits a long-range order, $\Delta_{\mathrm{CD}}(x)$ increases with x and converges to zero at $x\to\infty$. Furthermore, if $D_{\mathrm{CD}}(L/2;L)$ decays algebraically, $\Delta_{\mathrm{CD}}(x)$ converges to a finite negative value at $x\to\infty$. Figure 6 shows the data of $\Delta_{\mathrm{CD}}(x)$ as a function of x.[33] The results clearly suggest that there are parameter regions where $\Delta_{\mathrm{CD}}(x)$ increases with x. We take this behavior as an evidence of the CD phase.

Based on the above results we conclude that the CD phase emerges in a finite region in the $J_\perp$-$J_\times$ plane. The phase boundaries estimated from the results of the slope $\Delta_{\mathrm{CD}}(x)$ above are plotted in the phase diagram, see Fig. 9 in Sec. III D. We note that, as shown in the appendix, the bending-up behavior of the dimer operator in the log-log plots is also observed in the frustrated Heisenberg chain (which can also be viewed as the zigzag ladder), which is well known to exhibit the dimer phase for sufficiently large next-nearest-neighbor exchange J_2.[34–38] This observation provides us with an important check of the approach to the frustrated ladder Eq. (1) and supports our interpretation of the data in Figs. 4 and 6.

Although not expected from the RG analysis, we have also examined possibility of the SD order in the model. For this purpose, we have calculated the local SD operator,

$$D_{\mathrm{SD}}(n;L) = \sum_{j=1,2} (-1)^j (\langle \mathbf{S}_{j,n}\cdot\mathbf{S}_{j,n+1}\rangle - \langle \mathbf{S}_{j,n+1}\cdot\mathbf{S}_{j,n+2}\rangle), \tag{24}$$

in the frustrated ladder Eq. (1) with up to $L=96$ rungs. In the calculation of the SD operator, we have employed an open boundary condition with an extra spin at each edge, which selects one of the SD patterns and lifts the twofold degeneracy in the possible SD ground states. The results are presented in Fig. 7. We find that $D_{\mathrm{SD}}(L/2;L)$ bends downward in a log-log plot, indicating the exponential decay. [$D_{\mathrm{SD}}(L/2;L)$ for $J_\times=-0.2$ and $J_\perp=-0.41$, at which point we have found that the decay of the SD order is the slowest, exhibits a nearly linear behavior, but it actually bends down slightly.] We have performed the same calculation for a wide parameter regime and found that $D_{\mathrm{SD}}(L/2;L)$ decays exponentially in each gapped phase or, at most, decays algebraically at a transition point. We thus conclude that the SD phase is absent in the model Eq. (1) with ferromagnetic $J_\perp$ and $J_\times$.

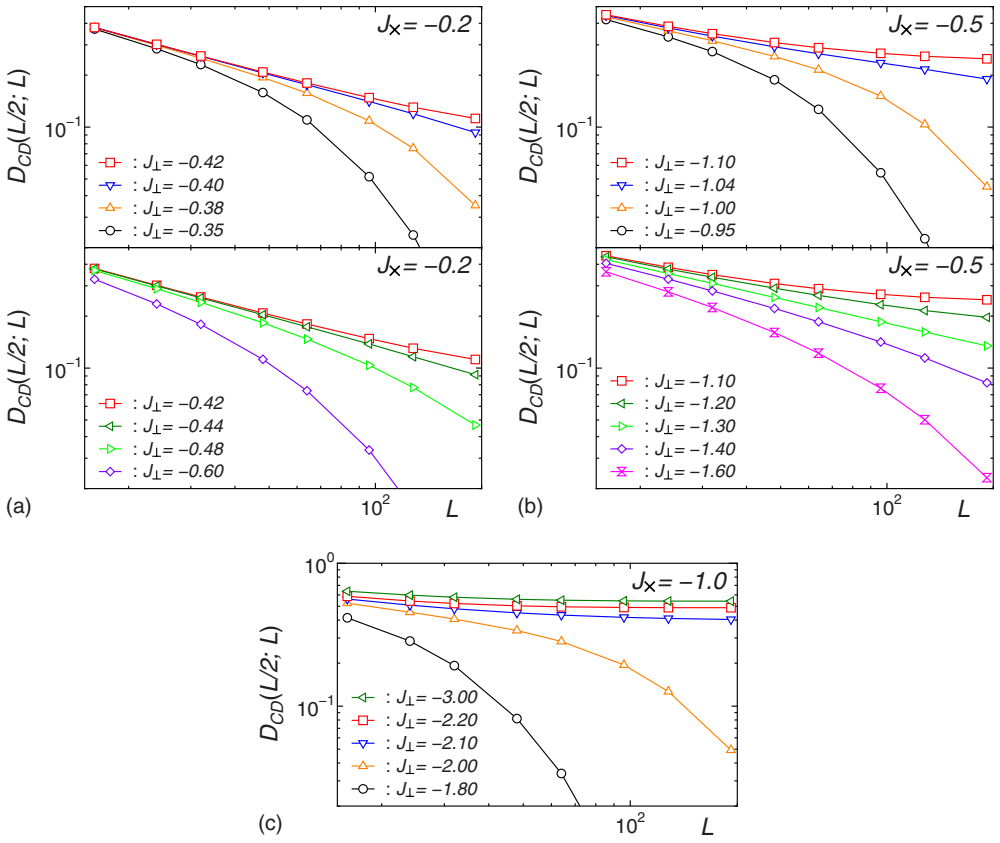

FIG. 4. (Color online) System-size dependence of the CD operator at the center of the open ladder, $D_{\mathrm{CD}}(L/2;L)$, in a log-log scale for $J=1$ and (a) $J_\times=-0.2$, (b) $J_\times=-0.5$, and (c) $J_\times=-1.0$.

C. z operator

Here, we discuss another numerical approach to the problem, based on so-called "z operators,"[39,40] which are used to distinguish different valence-bond-solid (VBS) states in one-dimensional spin systems. For the frustrated ladder model Eq. (1), two z operators, z_{rung} and z_{diag}, are defined as follows:

$$z_{\mathrm{rung}}(L) = \left\langle \exp\left[i\frac{2\pi}{L}\sum_{n=1}^{L} n(S^z_{1,n} + S^z_{2,n}) \right] \right\rangle,$$

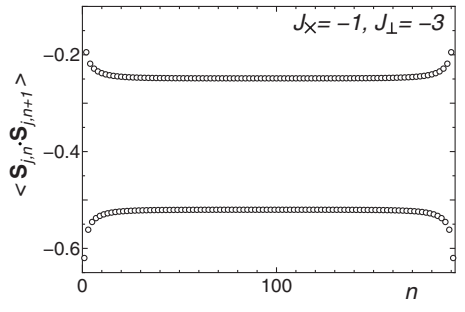

FIG. 5. Spin correlations between nearest-neighbor spins (bond energy) along the legs of the ladder, $\langle \mathbf{S}_{j,n} \cdot \mathbf{S}_{j,n+1} \rangle$, for $(J, J_\times, J_\perp) = (1, -1, -3)$ and $L=192$. The correlations in the legs $j=1$ and 2 are identical.

$$z_{\mathrm{diag}}(L) = \left\langle \exp\left[i\frac{2\pi}{L}\sum_{n=1}^{L} n(S^z_{1,n+1} + S^z_{2,n}) \right] \right\rangle. \quad (25)$$

It has been shown[39,40] that the z operators in the spin-1/2 two-leg ladder with L rungs under the periodic boundary condition exhibits the following asymptotic behavior with L:

$$z_{\mathrm{rung/diag}}(L) \sim (-1)^{N_{\mathrm{VBS}}}[1 - \mathcal{O}(1/L)], \quad (26)$$

where N_{VBS} is an integer depending on the VBS pattern of the state under consideration: it represents the number of singlet bonds "cut" by a line parallel to the rung/diagonal link. The z operator then measures topological parity of the dimer covering pattern describing particular gapped state. In our case, z_{rung} converges to 1 for the RS and CD states (even number of singlets crossed) in the thermodynamic limit, while $z_{\mathrm{rung}} \to -1$ for the Haldane state (the number of crossed singlets is always odd). Conversely, $z_{\mathrm{diag}} \to -1$ for the RS and CD states, while $z_{\mathrm{diag}} \to 1$ in the Haldane state. A remarkable feature of the z operators is that they change their sign at the transition between phases having different parity of N_{VBS}. This property makes the z operators more powerful in determining the critical point of such a phase transition than the string order parameter, which just vanishes at the transition.[20] Indeed, the z operators have turned out to be successful in determining the direct RS-Haldane transition point occurring for large antiferromagnetic $J_{\perp,\times}$.[40] For the present case of ferromagnetic $J_{\perp,\times}$, we can use z_{rung} and z_{diag} to locate the

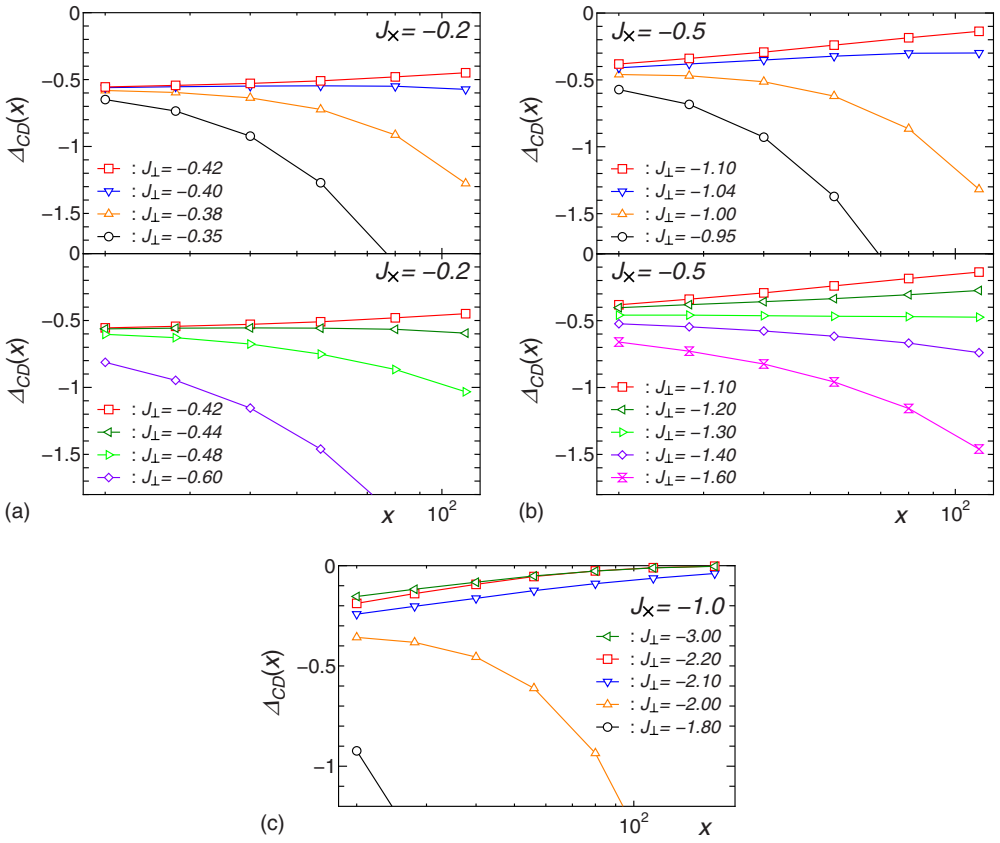

FIG. 6. (Color online) Slope of the log $D_{\mathrm{CD}}(L/2;L)$ − log L plot, $\Delta_{\mathrm{CD}}(x)$, for $J=1$ and (a) $J_\times=-0.2$, (b) $J_\times=-0.5$, and (c) $J_\times=-1.0$.

transition point between the CD and Haldane phases.

Using the exact-diagonalization method, we have calculated the z operators, z_{rung} and z_{diag}, in the ladder Eq. (1) with up to $L=12$ rungs under the periodic boundary condition. Figure 8 presents the results for typical parameter lines with $J=1$ and fixed $J_\times$. For $J_\times<1$, we have observed the sign change in z_{rung} (z_{diag}) from positive (negative) to negative (positive) values as $J_\perp$ decreases. The crossing point of z_{rung} and z_{diag} thereby gives an estimate of the transition point between the CD and Haldane phases. While the L dependence is negligibly small for small $|J_\times|$, the crossing point for large $|J_\times|$ moves sizably with L, suggesting that the finite-size effects still remain. However, we emphasize that the crossing point shifts toward smaller $J_\perp$ with increasing L,

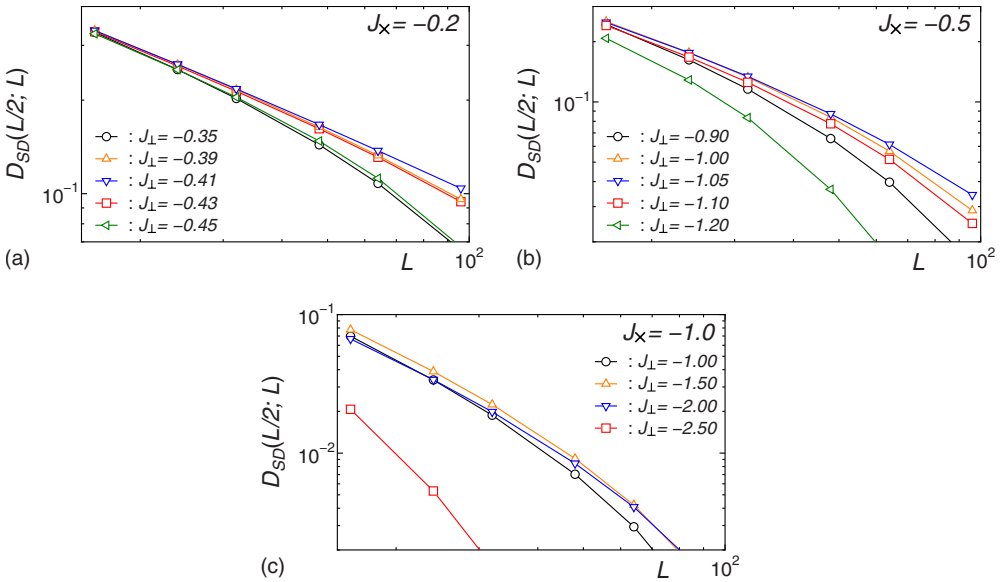

FIG. 7. (Color online) System-size dependence of the SD operator at the center of the open ladder, $D_{\mathrm{SD}}(L/2;L)$, in a log-log scale for $J=1$ and (a) $J_\times=-0.2$, (b) $J_\times=-0.5$, and (c) $J_\times=-1.0$.

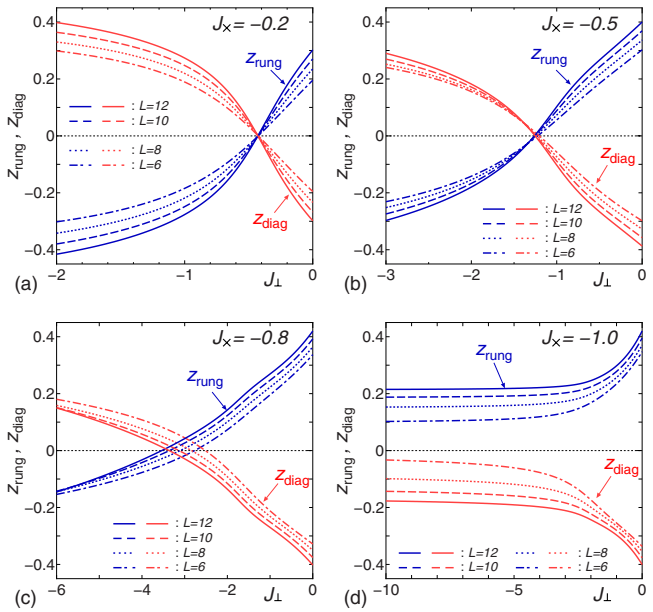

FIG. 8. (Color online) $J_\perp$ dependence of the z operators for $J=1$ and (a) $J_\times=-0.2$, (b) $J_\times=-0.5$, (c) $J_\times=-0.8$, (d) $J_\times=-1.0$. Dark (blue) and light (red) curves represent z_{rung} and z_{diag}, respectively.

which means that the range of CD phase *broadens* as L increases, and approaches smoothly to the CD-Haldane transition point obtained from the DMRG analysis. (See also the phase diagram, Fig. 9 in Sec. III D.) Thus, we can safely state that the analysis of z operators also supports the appearance of the CD phase. For $J_\times=1$, z_{rung} (z_{diag}) is positive (negative) for the entire regime of $J_\perp$ calculated. The result is consistent with the prediction of the perturbative analysis in Sec. III A as well as the DMRG results in Sec. III B, which show that the CD phase extends to the limit $J_\perp \to -\infty$.

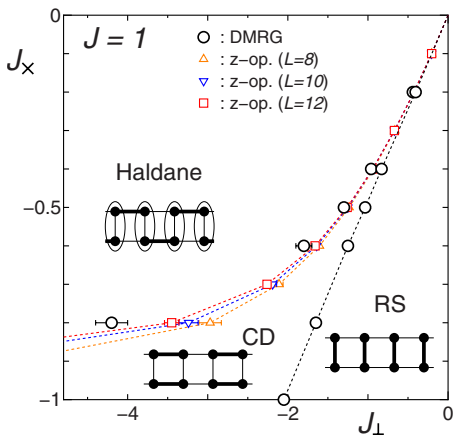

FIG. 9. (Color online) Ground-state phase diagram for $J=1$ and the ferromagnetic interchain coupling, $J_\perp<0$ and $J_\times<0$. Open circles represent the transition points obtained from the DMRG calculation while the other symbols show the CD-Haldane transition points from the analysis of z operators. Dotted lines are guide to eyes. In the schematic pictures for each phase, the bold lines represent singlet pairs and the ellipses stand for the symmetrization of two spins.

D. Phase diagram

Combining the above results, we determine the ground-state phase diagram in the parameter plane for ferromagnetic $J_\perp$ and $J_\times$. Figure 9 shows the resultant phase diagram, which includes the Haldane, RS, and CD phases. We clearly see that the CD phase appears in a wide parameter region, which is seen to expand as $|J_\perp|$ and $|J_\times|$ become bigger. The transition line between the RS and CD phases seems to nearly coincide with the line of $J_\perp=2J_\times$. The boundary between the Haldane and CD phases starts from $J_\perp=J_\times=0$ and runs toward smaller $J_\perp$ as $J_\times$ decreases, approaching smoothly the limit of the strong rung exchange, $J_\times=-J$ at $J_\perp \to -\infty$. It is worth noting that the DMRG result on the RS-CD transition line agrees even quantitatively with the result of RG analysis in Table I, and the behavior of the CD-Haldane transition line is also consistent with the analytical RG result. This observation strongly supports the correctness of the RG analysis in Sec. II.

IV. ANTIFERROMAGNETIC INTERCHAIN COUPLINGS

The numerical results in Sec. III have revealed that the frustrated ladder Eq. (1) with ferromagnetic $J_\perp$ and $J_\times$ exhibits the CD phase in a wide parameter regime, in agreement with the prediction of RG analysis in Sec. II. Since the validity of the RG analysis relies only on the small amplitudes of the interchain couplings $J_\perp$ and $J_\times$ and is not affected by their signs, we naturally expect that the RG analysis is correct also for the antiferromagnetic couplings. To examine the expectation, we revisit the frustrated ladder Eq. (1) with antiferromagnetic $J_\perp$ and $J_\times$. For this case, it has been shown rather clearly that for large $J_\perp$ and $J_\times$ the direct first-order transition takes place between the RS and Haldane phases,[15] while the situation is still controversial for small $J_\perp$ and $J_\times$.[14–16] To clarify the situation we have performed the DMRG calculation for a parameter line $J=1$ and $J_\times=0.2$ and investigated behaviors of the CD and SD operators.

Figures 10 and 11 show the system-size dependence of the CD and SD operators at the center of the open ladder, $D_{\mathrm{CD}}(L/2;L)$ and $D_{\mathrm{SD}}(L/2;L)$, and the slopes of their log-log plots, $\Delta_{\mathrm{CD}}(x)$ and $\Delta_{\mathrm{SD}}(x)$, respectively.[33,41] [$\Delta_{\mathrm{SD}}(x)$ is defined in the same way as Eq. (23).] We note that our data of the CD operator $D_{\mathrm{CD}}(L/2;L)$ for $J_\perp \le 0.37$ and $J_\perp \ge 0.39$ coincide with the results shown in Ref. 14, while the data for $J_\perp=0.38$ was not presented there. We find in Fig. 10 that both $D_{\mathrm{CD}}(L/2;L)$ and $D_{\mathrm{SD}}(L/2;L)$ decay exponentially with L for $J_\perp \le 0.37$ (Haldane phase) and $J_\perp \ge 0.39$ (RS phase), suggesting the absence of the CD and SD orders in the parameter regions. On the other hand, it is remarkable that for $J_\perp=0.38$ the CD operator $D_{\mathrm{CD}}(L/2;L)$ bends upward in the log-log plot, indicating the emergence of the CD long-range order. The tendency toward the CD ordering is elucidated also in Fig. 11(a), which shows that the slope of the $\log D_{\mathrm{CD}}(L/2;L)-\log L$ plot, $\Delta_{\mathrm{CD}}(x)$, increases with x. We note that, in contrast to the CD operator, the SD operator $D_{\mathrm{SD}}(L/2;L)$ exhibits the bending-down behavior in the log-log plot even for $J_\perp=0.38$. The opposite trends of the CD and SD operators imply that the growth of the CD order observed at $J_\perp=0.38$ is not a critical enhancement at a tran-

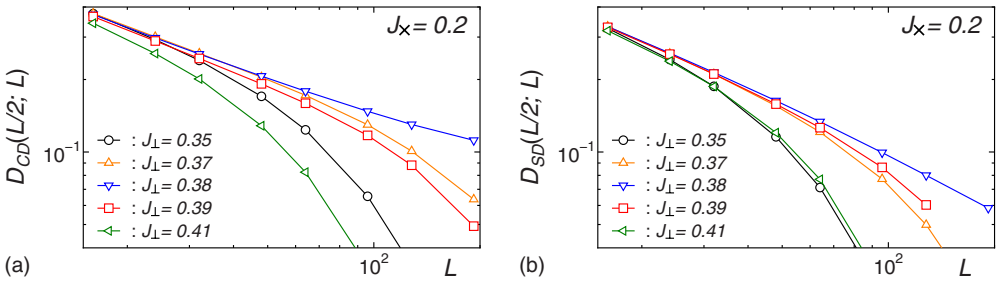

FIG. 10. (Color online) System-size dependence of the dimer operators at the center of the open ladder in a log-log scale for $J=1$ and $J_\times=0.2$; (a) the CD operator $D_{\mathrm{CD}}(L/2;L)$ and (b) the SD operator $D_{\mathrm{SD}}(L/2;L)$.

sition point but an indication of a true CD long-range order. We therefore expect that the CD phase appears in a narrow but finite-parameter region around $J_\perp=0.38$, in accordance with the RG prediction[13] and the discussion in Sec. II, and in agreement with recent numerical finding in Ref. 16.

V. DISCUSSION

The main result of our study is the discovery of the columnar dimer phase in the frustrated ladder problem with *ferromagnetic* interchain interactions, see Fig. 9. This finding, confirmed by extensive DMRG analysis in Sec. III B, is based on analytic RG arguments summarized in Sec. II. It confirms novel mechanism of dimerization by frustrated interchain couplings, proposed in Ref. 13. Previous sightings of the spontaneously dimerized state, of either columnar or staggered type, were restricted to models with four-spin interaction terms, such as the ring-exchange model and the $\mathrm{SU}(2)\times\mathrm{SU}(2)$ ladder.[3,42–47]

The success of this study in describing ferromagnetic interleg exchanges gives us confidence in essential validity of the weak-coupling RG approach and makes it possible to revisit the more complicated case of *antiferromagnetic* interleg exchanges, as described in Sec. IV. There we also find hints of developed CD order at $(J,J_\times,J_\perp)=(1,0.2,0.38)$, in agreement with Ref. 16. The extent of the CD region is very narrow: finite-size scaling analysis in Ref. 16 estimates that $0.373\leq J_\perp\leq 0.386$ for $J_\times=0.2$. Such a limited range may explain negative results of the two previous studies.[14,15]

In addition to these numerical observations our work takes important step forward in uncovering the reason for the more narrow than naively expected, on the basis of the estimate Eq. (5), range of existence of the CD order. That feature, as we argue in Sec. II, has to do with marginally relevant character of the current-current interaction between spin chains in the case of antiferromagnetic interleg exchanges. We predict that the CD phase ceases to exist at all once interleg exchange $J_\times$ exceeds the critical value of the order 0.3. Connecting this CD phase with the dimerized phases of frustrated two-dimensional spin models (see Ref. 48 for the original large-N study and Ref. 49 for recent developments) represents an important outstanding problem.

Before concluding we would like to note that there exists another simple route to the dimerized phase. It consists in turning marginally irrelevant in-chain backscattering G_5 into a marginally relevant one.[50] This is achieved by introducing sufficiently strong antiferromagnetic coupling J_2 between next-nearest spins along the legs of the ladder. Provided that it exceeds the critical value,[17] $J_2>0.241J$, the legs of the ladder will be spontaneously dimerized even in the absence of any interchain coupling. The remaining weak interchain interactions then work to stabilize one of the two ordered dimerization patterns, columnar or staggered, as is described in Ref. 50 and observed in Ref. 16. Connecting this large-J_2 regime with the case studied here represents another interesting topic we leave for future.

ACKNOWLEDGMENTS

It is our pleasure to acknowledge numerous stimulating discussions with Leon Balents. We would like to thank A. Honecker, A. Furusaki, A. Nersesyan, and J. Sólyom for useful conversations. This work was supported by Grants-in-Aid for Scientific Research from the Ministry of Education, Culture, Sports, Science and Technology (MEXT) of Japan, Grant No. 21740277 (T.H.), and by the NSF, Grant No. DMR-0808842 (O.A.S.).

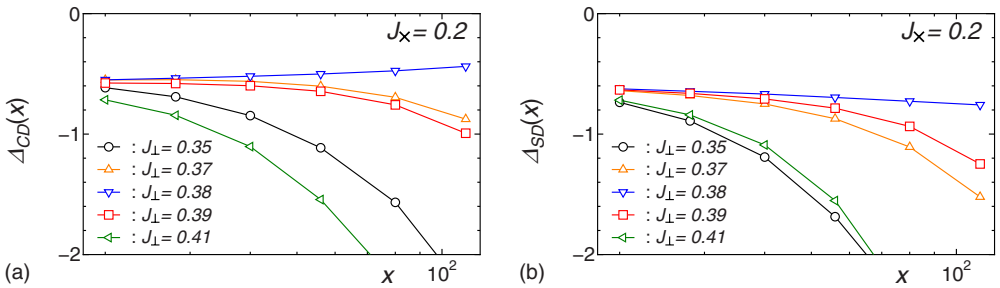

FIG. 11. (Color online) Slope of the log-log plots of the dimer operators for $J=1$ and $J_\times=0.2$; (a) $\Delta_{\mathrm{CD}}(x)$ and (b) $\Delta_{\mathrm{SD}}(x)$.

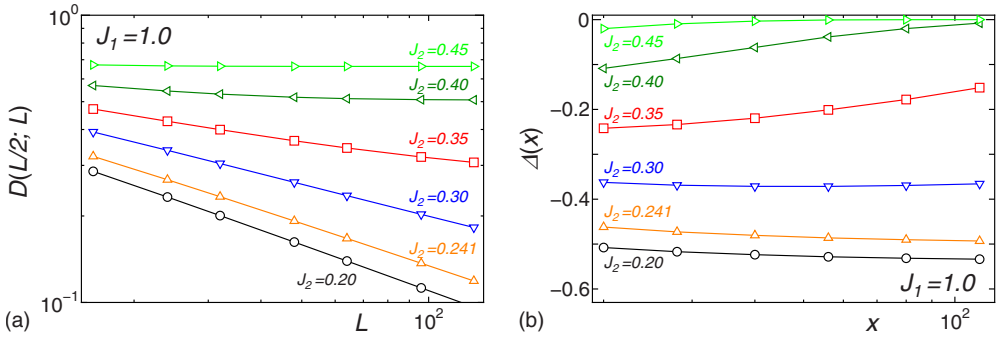

FIG. 12. (Color online) DMRG data for the dimer operator in the J_1-J_2 chain with $J_1=1$; (a) dimer operator $D(L/2;L)$ at the center of the open chain and (b) slope of the log $D(L/2;L)-\log L$ plot, $\Delta(x)$. The symbols represent the results for $J_2=0.20$, 0.241, 0.30, 0.35, 0.40, and 0.45 from bottom to top.

APPENDIX: DIMER ORDER IN J_1-J_2 CHAIN

In this appendix, we check the behavior of the dimer operator in a finite open spin chain as a function of chain length. To this end, we consider well-understood frustrated Heisenberg chain (J_1-J_2 model),

$$H_{\text{zig}} = J_1 \sum_n \mathbf{S}_n \cdot \mathbf{S}_{n+1} + J_2 \sum_n \mathbf{S}_n \cdot \mathbf{S}_{n+2}, \tag{A1}$$

where $\mathbf{S}_n$ is the spin-1/2 operator at the nth site and J_1 and J_2 are coupling constants of the nearest- and next-nearest-neighbor exchange interactions, respectively. It is well established that in the case of antiferromagnetic couplings, $J_1, J_2 > 0$, the J_1-J_2 chain [Eq. (A1)] exhibits a critical (Luttinger-liquid) phase for $J_2/J_1 < (J_2/J_1)_c = 0.241$, while for $J_2/J_1 > (J_2/J_1)_c$ the ground state is spontaneously dimerized.[17,34–38]

Using the DMRG method, we calculate the dimer operator,

$$D(n;L) = \langle \mathbf{S}_n \cdot \mathbf{S}_{n+1} - \mathbf{S}_{n+1} \cdot \mathbf{S}_{n+2} \rangle, \tag{A2}$$

in the chain with up to $L=128$ spins under the open boundary condition. Figure 12 shows the system-size dependence of the dimer operator at the center of the chain, $D(L/2;L)$, and its slope in the log-log plot, $\Delta(x)$, for several typical values of J_2/J_1. [The slope $\Delta(x)$ is defined as in Eq. (23).] For $J_2/J_1 < 0.241$, where the model is in the critical phase, the dimer operator $D(L/2;L)$ decays algebraically with L, as expected. For $0.241 < J_2/J_1 \lesssim 0.3$, for which regime it is known that the system is in the dimer phase but the spin gap is exponentially small, the dimer operator seemingly decays in a power law. This can be understood as a consequence of the fact that the correlation length is so large that we cannot reach the asymptotic behavior of the dimer operator within the system size treated, $L \leq 128$. For $J_2/J_1 \gtrsim 0.35$, deep in the dimer phase, $D(L/2;L)$ shows the bending-up behavior in the log-log scale, and eventually, the dimer long-range order is clearly observed for $J_2/J_1=0.45$.

The results indicate that the bending-up behavior of the dimer operator in the log-log plot is observed only in the dimer phase and when the system size is comparable to or larger than the correlation length. We can therefore safely regard the bending-up behavior as an evidence of the dimer ordering.

[1] *Frustrated Spin Systems*, edited by H. T. Diep (World Scientific, Singapore, 2005).
[2] D. G. Shelton, A. A. Nersesyan, and A. M. Tsvelik, Phys. Rev. B **53**, 8521 (1996).
[3] A. A. Nersesyan and A. M. Tsvelik, Phys. Rev. Lett. **78**, 3939 (1997).
[4] J.-B. Fouet, F. Mila, D. Clarke, H. Youk, O. Tchernyshyov, P. Fendley, and R. M. Noack, Phys. Rev. B **73**, 214405 (2006).
[5] J. S. Meyer and K. A. Matveev, J. Phys.: Condens. Matter **21**, 023203 (2009).
[6] D. N. Sheng, O. I. Motrunich, S. Trebst, E. Gull, and M. P. A. Fisher, Phys. Rev. B **78**, 054520 (2008).
[7] U. Schollwöck, Rev. Mod. Phys. **77**, 259 (2005).
[8] K. A. Hallberg, Adv. Phys. **55**, 477 (2006).
[9] E. Dagotto, Rep. Prog. Phys. **62**, 1525 (1999).
[10] S. Notbohm, P. Ribeiro, B. Lake, D. A. Tennant, K. P. Schmidt, G. S. Uhrig, C. Hess, R. Klingeler, G. Behr, B. Büchner, M. Reehuis, R. I. Bewley, C. D. Frost, P. Manuel, and R. S. Eccleston, Phys. Rev. Lett. **98**, 027403 (2007).
[11] B. Lake, Alexei M. Tsvelik, Susanne Notbohm, D. Alan Tennant, Toby G. Perring, Manfred Reehuis, Chinnathambi Sekar, Gernot Krabbes, and Bernd Büchner, Nat. Phys. **6**, 50 (2010).
[12] I. A. Zaliznyak, C. Broholm, M. Kibune, M. Nohara, and H. Takagi, Phys. Rev. Lett. **83**, 5370 (1999).
[13] O. A. Starykh and L. Balents, Phys. Rev. Lett. **93**, 127202 (2004).
[14] H. H. Hung, C. D. Gong, Y. C. Chen, and M. F. Yang, Phys. Rev. B **73**, 224433 (2006).
[15] E. H. Kim, Ö. Legeza, and J. Sólyom, Phys. Rev. B **77**, 205121 (2008).
[16] G. H. Liu, H. L. Wang, and G. S. Tian, Phys. Rev. B **77**, 214418 (2008).

[17] S. Eggert, Phys. Rev. B **54**, R9612 (1996).
[18] A. A. Nersesyan, A. O. Gogolin, and F. H. L. Essler, Phys. Rev. Lett. **81**, 910 (1998).
[19] D. Allen, F. H. L. Essler, and A. A. Nersesyan, Phys. Rev. B **61**, 8871 (2000).
[20] E. H. Kim, G. Fáth, J. Sólyom, and D. J. Scalapino, Phys. Rev. B **62**, 14965 (2000).
[21] A. A. Nersesyan and A. M. Tsvelik, Phys. Rev. B **67**, 024422 (2003).
[22] M. Nakamura, J. Phys. Soc. Jpn. **68**, 3123 (1999).
[23] M. Nakamura, Phys. Rev. B **61**, 16377 (2000).
[24] M. Tsuchiizu and A. Furusaki, Phys. Rev. Lett. **88**, 056402 (2002).
[25] J. B. Parkinson, J. Phys. C **20**, L1029 (1987).
[26] J. B. Parkinson, J. Phys. C **21**, 3793 (1988).
[27] M. N. Barber and M. T. Batchelor, Phys. Rev. B **40**, 4621 (1989).
[28] A. Klümper, Europhys. Lett. **9**, 815 (1989).
[29] I. Affleck, J. Phys.: Condens. Matter **2**, 405 (1990).
[30] Y. Xian, Phys. Lett. A **183**, 437 (1993).
[31] S. R. White, Phys. Rev. Lett. **69**, 2863 (1992).
[32] S. R. White, Phys. Rev. B **48**, 10345 (1993).
[33] In Figs. 6(a), 6(b), and 11, the data of the slope $\Delta_{\mathrm{CD/SD}}(x)$ for $x=x_7=160$ are not shown since the truncation error of the DMRG calculation, which is amplified by the numerical derivative in Eq. (23), is not negligible for these cases.
[34] C. K. Majumdar and D. K. Ghosh, J. Math. Phys. **10**, 1388 (1969).
[35] C. K. Majumdar and D. K. Ghosh, J. Math. Phys. **10**, 1399 (1969).
[36] F. D. M. Haldane, Phys. Rev. B **25**, 4925 (1982).
[37] R. Jullien and F. D. M. Haldane, Bull. Am. Phys. Soc. **28**, 344 (1983).
[38] K. Okamoto and K. Nomura, Phys. Lett. A **169**, 433 (1992).
[39] M. Nakamura and S. Todo, Phys. Rev. Lett. **89**, 077204 (2002).
[40] M. Nakamura and S. Todo, Prog. Theor. Phys. Suppl. **145**, 217 (2002).
[41] In Fig. 10(b), the SD operator $D_{\mathrm{SD}}(L/2;L)$ for $J_\perp=0.39$ and $L=192$ is not shown as the DMRG calculation was not stable in this case. We note that this feature can be naturally understood within the VBS picture as the boundary condition with additional edge spins, employed in the calculation of the SD operator, is not compatible with the RS ground state realized at this parameter point. In the RS ground state these additional edge spin-1/2 moments essentially decouple from the bulk and spoil numerical stability of the calculation. Similar effect is well known in the Haldane phase where the free-edge moments are induced in the ladder under the simple open boundary condition. We have observed this phenomenon in the wide range of exchange parameters corresponding to the RS, CD, and Haldane phases.
[42] A. K. Kolezhuk and H.-J. Mikeska, Phys. Rev. Lett. **80**, 2709 (1998).
[43] A. K. Kolezhuk and H.-J. Mikeska, Int. J. Mod. Phys. B **12**, 2325 (1998).
[44] S. K. Pati, R. R. P. Singh, and D. I. Khomskii, Phys. Rev. Lett. **81**, 5406 (1998).
[45] M. Müller, T. Vekua, and H.-J. Mikeska, Phys. Rev. B **66**, 134423 (2002).
[46] A. Läuchli, G. Schmid, and M. Troyer, Phys. Rev. B **67**, 100409(R) (2003).
[47] T. Momoi, T. Hikihara, M. Nakamura, and X. Hu, Phys. Rev. B **67**, 174410 (2003).
[48] N. Read and S. Sachdev, Phys. Rev. B **42**, 4568 (1990).
[49] A. Ralko, M. Mambrini, and D. Poilblanc, Phys. Rev. B **80**, 184427 (2009).
[50] T. Vekua and A. Honecker, Phys. Rev. B **73**, 214427 (2006).